

Loss Bounds for Approximate Influence-Based Abstraction

Elena Congeduti
Computer Science
Delft University of Technology
E.Congeduti@tudelft.nl

Alexander Mey
Computer Science
Delft University of Technology
A.Mey@tudelft.nl

Frans A. Oliehoek
Computer Science
Delft University of Technology
F.A.Oliehoek@tudelft.nl

ABSTRACT

Sequential decision making techniques hold great promise to improve the performance of many real-world systems, but computational complexity hampers their principled application. Influence-based abstraction aims to gain leverage by modeling local subproblems together with the ‘influence’ that the rest of the system exerts on them. While computing exact representations of such influence might be intractable, learning approximate representations offers a promising approach to enable scalable solutions. This paper investigates the performance of such approaches from a theoretical perspective. The primary contribution is the derivation of sufficient conditions on approximate influence representations that can guarantee solutions with small value loss. In particular we show that neural networks trained with cross entropy are well suited to learn approximate influence representations. Moreover, we provide a sample based formulation of the bounds, which reduces the gap to applications. Finally, driven by our theoretical insights, we propose approximation error estimators, which empirically reveal to correlate well with the value loss.

KEYWORDS

Sequential decision making, Multiagent systems, Best-response problems, State abstraction, Learning abstractions, Loss bounds.

1 INTRODUCTION

Sequential decision making methods have the potential to improve control in distributed or networked systems that can involve many agents and complex environments. However, applying these methods in a principled manner is often difficult due to computational complexity. One idea to try to improve scalability is using abstractions, compressed representations of the sufficient information for an agent to perform optimal decisions. Many abstraction approaches have been suggested [2, 14, 16, 23] but in order to ensure small value loss, they only allow abstracting states of the environment with similar dynamics. A body of work on localized abstractions [3, 5, 40, 48] tries to overcome this issue, allowing to abstract large part of the system away. These approaches leverage the sparse interaction structures of many real-world domains where the agent’s reward and observations depend directly only on few (local) state variables.

Influence-based abstraction (IBA) [35] generalizes over these approaches and provides a unified framework for localized abstractions for a general class of multiagent problems. The basic idea is to decompose structured multiagent systems into small submodels for each agent where only few local variables are included. The ‘influence’ summarizes the indirect effects of other agents policies and the rest of the environment on the local variables of a single

agent. Since the decision maker can avoid reasoning about the entire problem, the best-response problem can be solved much more efficiently in the abstract local model without any loss in value. This approach may not only enable speedups in best-response problems but serves also as foundation for scalable multiagent approaches based, for instance, on searching in the space of influences [48].

However, even though IBA provides a lossless abstraction, in general, deducing an *exact representation* of the influence itself is computationally intractable even for simple problems. Given the rapid progress in learning methods for sequence prediction [1, 20, 22], we envision that inducing *approximate representations* of the influence offers a promising approach to scalable solutions. This raises a fundamental question. To what extent are such existing methods (and their proxy-loss functions) aligned with the actual objective of influence-based abstraction: achieving near-optimal value?

In this work we address this issue, showing that there is theoretical and empirical evidence that employing existing sequence predictors can lead to good approximate influence representations. In particular, we derive a performance loss bound as well as a probabilistic version that provides quality guarantees on approximate influence to ensure near-optimal solutions. Like bounds based on the Bellman error, our bounds themselves are computationally intractable for large problems. This is to be expected: the performance loss is characterized by the quality of each possible prediction. Therefore, deriving an exact bound essentially corresponds to computing the exact generalization error of the employed machine learning model. Nevertheless, we show that a neural network trained with cross-entropy loss seems well suited for the prediction task, as the training objective is aligned with the bound we derived. Finally, we empirically demonstrate that it is possible to compute statistics, based on the empirical test error of approximate influence, that correlate well with the actual value loss.

In summary, our contributions in this paper are:

- (1) Sufficient conditions for goodness of approximation of influence in terms of value loss.
- (2) Discussing how these conditions are aligned with usual optimization of neural networks trained with cross entropy loss.
- (3) An empirical evaluation that demonstrates that optimizing cross entropy loss of influence predictors indeed leads to lower performance loss in the sequential decision making problem.

2 BACKGROUND

2.1 Sequential Decision Making Framework

We consider a general class of multiagent problems that can be modeled as partially observable stochastic games (POSG). [18].

Definition 1 (POSG). A *Partially Observable Stochastic Game* is a tuple $M = (n, S, A, O, T, \Omega, R, h, b^0)$ where n agents interact in the

finite state space S . $A = A_1 \times \dots \times A_n$ and $O = O_1 \times \dots \times O_n$ are the finite spaces of joint actions and observations respectively. T models the transition probabilities as $T(s'|s, a) = \mathbb{P}(s'|s, a)$, namely the probability of resulting in state s' when actions $a = (a_1, \dots, a_n)$ are chosen in state s . Ω is the observation distribution, $\Omega(o'|a, s') = \mathbb{P}(o'|a, s')$, that is, the probability of receiving observations $o = (o_1, \dots, o_n)$ when performing actions a results in state s' . $R(s, a) = (R_1(s, a), \dots, R_n(s, a))$ represent the immediate reward functions for each agent for taking actions a in state s . Finally, h defines the horizon of the process and b^0 the initial state distribution.

In a POSG, each agent i employs a policy, π_i that corresponds to a possibly stochastic map from the action-observation history to the action space. A joint policy $\pi = (\pi_1, \dots, \pi_n)$ is a tuple of policies for each of the agents. Given a joint policy π , we can define the corresponding expected cumulative reward function for an agent i :

$$V_i^\pi = \mathbb{E} \left[\sum_{t=1}^h R_i^t \mid \pi, b^0 \right].$$

Different optimization problems and corresponding solution concepts can be considered according to the adversarial or cooperative nature of the agents. In the first case, the problem consists of searching for Nash equilibria (NE), joint policies $\pi = (\pi_i, \pi_{-i})$ such that each agent i draws no advantage from deviating from its policy π_i given the policies of the others π_{-i} . In cooperative settings modeled by decentralized partially observable Markov decision processes (Dec-POMDPs) [7, 30], the solution consists of finding the optimal join policy π maximizing the value function shared by all players. Many solutions methods for searching NE as fictitious play [6, 11], double oracle [25], parallel Nash memory [32] and for optimal policies for Dec-POMDPs as influence search [48] use best-response computations as their inner loop. A best response π_i^* for agent i against a fixed tuple of policies π_{-i} for the other agents is the policy maximizing the value function $\max_{\pi_i} V_i^{(\pi_i, \pi_{-i})}$.

However, computing best-responses implies reasoning over the entire state space and other agents action-observation histories [27]. To ease this task we want to exploit the structural properties of the environment to build local abstractions for best-response problems. Frequently, in fact, the state space can be thought as composed of different state variables, or *factors* [10]. In this case, the model is called *factored POSG* and the state space can be represented as $S = X_1 \times \dots \times X_m$. This structure allows to decompose the system into (weakly) coupled subproblems, *local models*, for single agents including only few factors. Thus, the idea is to define an equivalent problem to the best response in which the agent needs only to reason over the local factors.

2.2 Influence-based abstraction

Influence-based abstraction [35] formalizes the concept of the local model for one agent and provides the formal framework to define the local abstraction for the best-response problem. Conceptually, the local model consists of all the observable factors that can fully determine the agent observations and rewards together with the influence that the rest of the system and other agents policies exert on it.

We will use capital letters to denote variables and small letters for variable instantiations. To simplify our discussion, we will restrict to locally fully-observable POSGs [17]

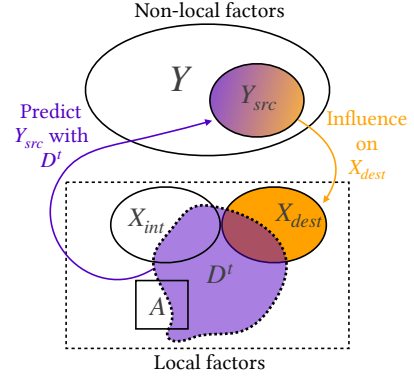


Figure 1: Depiction of a local model. Local factors are given by X_{int} and X_{dest} , while non-local factors by Y . The orange part depicts the direct influence of $Y_{\text{src}} \subset Y$ on X_{dest} . In order to accommodate for Y_{src} we remember the history of a subset of relevant local variables, denoted by D^t , where t indicates the current time step. Here D^t can include variables from X_{int} , X_{dest} and also the local action A . The purple part depicts the idea of predicting Y_{src} with D^t .

Definition 2 (Fully Observable Local Model). In a factored POSG, a *Fully Observable Local Model* for one agent is a subset of fully observable state variables, called the *local factors*, including all the factors directly affecting the observations and reward. We denote the local state, the collection of all the local factors, as X and the complementary collection of *non-local factors* as Y , such that the state space can be partitioned as $S = X \times Y$. We further distinguish between local factors X_{dest} that are directly affected by non-local variables, called *influence destinations*, and local factors X_{int} whose dynamic is only affected internally by other local factors. Thus, the local state X can be decomposed as $X = (X_{\text{int}}, X_{\text{dest}})$. We refer to the non-local variables $Y_{\text{src}} \subset Y$ that directly exert an influence on the local model as the *influence sources*.

When abstracting away the non-local factors Y , the dynamics of X_{dest} become non-Markovian. Accordingly, the local state transitions are not well defined. To define the local state dynamics, we need to include as part of the local state space the history of relevant local actions and factors to infer the external influence Y_{src} . The notion of *d-separating set* (d-set) [9] formalizes this concept. That is, the d-set at time t , D^t contains the histories of the relevant local factors and actions necessary to predict the influence sources Y_{src}^t .

Figure 1 provides a graphical depiction of the distinction between the local and non-local variables, the d-separating set, and the dynamics between all of them. Note that once the other agents policies are fixed, their actions become random variables that we can compactly represent as non-local factors.

Definition 3 (Influence Point). The *exact influence point* (EIP) $I = (I^0, \dots, I^{h-1})$ is a collection of conditional probability distributions $I^t(Y_{\text{src}}^t | D^t) \triangleq \mathbb{P}(Y_{\text{src}}^t | D^t, \pi_{-i}, b^0)$ of the influence sources Y_{src}^t given the possible instantiations of the d-set.

The intuition of the local model is formalized by the *influence-augmented local model* (IALM), a factored Markov decision process

(MDP) where the state space consists of a local state augmented with the d-set.

Definition 4 (Influence Augmented Local Model). In a factored POSG $M = (n, S, A, O, T, \Omega, R, h, b^0)$, given a fully observable local model for agent i and fixed policies for the other agents π_{-i} , an *Influence Augmented Local Model* (IALM) $\mathcal{M}_i = (\tilde{S}_i, A_i, \tilde{T}_i, R_i, h, b^0)$ is a factored MDP where the action space A_i and rewards R_i correspond to the POSG agent i 's actions and rewards. The augmented state space \tilde{S}_i consists of tuples of local states and d-separating sets, $\tilde{S}^t = (X^t, D^t) = ((X_{\text{int}}^t, X_{\text{dest}}^t), D^t)$. The transition functions for every state \tilde{s}^t , \tilde{s}^{t+1} and action a^t are derived as follows

$$\mathcal{T}_i(\tilde{s}^{t+1}|\tilde{s}^t, a^t) = T(x_{\text{int}}^{t+1}|x^t, a^t) \sum_{y_{\text{src}}^t} T(x_{\text{dest}}^{t+1}|x^t, y_{\text{src}}^t, a^t) I^t(y_{\text{src}}^t|d^t). \quad (1)$$

This model defines an equivalent problem to the best-response problem for an agent i . That is, the optimal policy for the MDP defined by the IALM \mathcal{M}_i for agent i corresponds to the best-response against policies π_{-i} in the factored POSG M . See [34] for the details.

2.3 Influence in Planetary Exploration

To give a concrete intuition of influence-based abstraction we use a version of the planetary exploration environment [48]. A rover has to explore a planet, and its navigation may be guided by a plan from a satellite. The goal of the rover is to move until it reaches a target site, where it will collect a positive reward. However, any time it fails to step forward it will receive a penalty. The satellite might help the rover by providing a plan which increases the likelihood of a successful step.

Figure 2 shows a dynamic Bayesian network (DBN) [10] that compactly represents the problem. At each time t the rover can observe its position pos and if a plan pl was available at the previous time step. The rover's local state consists of $X = (pos, pl)$. The plan pl is the influence destination since it is directly affected by the non-local satellite action a_{sat} which is the influence source. Contrarily, the position pos is only directly affected by local variables.

The decisions of the satellite might depend on its level of battery, the *charge*, which only indirectly affects the local model through the satellite's actions. Potentially, the decision-making problem of the satellite might depend on a conceivably larger number of variables: it has to manage its own resources, send plans to other rovers etc. However, the only information the rover needs to retrieve to act optimally is whether the satellite will make available a routing plan at the next step. Therefore, it can abstract away all the other state variables and try to *predict* the satellite's action, given all the relevant information that it has in the local model. In this scenario, it turns out that all it has to remember is the history of the availability of plans at each time step. Therefore the influence point consists of the distribution of the satellite's actions $Y_{\text{src}}^t = a_{\text{sat}}^t$, given the local history of the plan $D^t = (pl^1, \dots, pl^t)$.

3 PLANNING WITH APPROXIMATE INFLUENCE REPRESENTATIONS

IBA has the potential to enable faster planning in complex domains where using the entire model would typically be too heavy and computational demanding with no information loss. However,

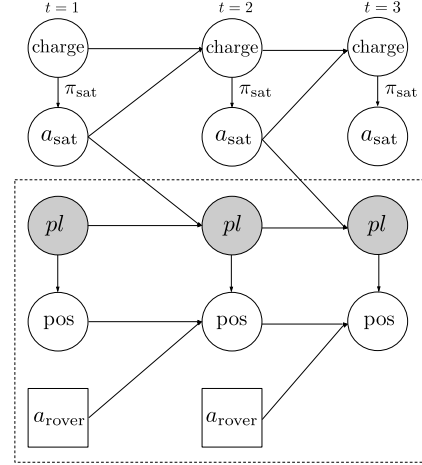


Figure 2: A DBN of the planetary exploration domain. The dotted square refers to the local model of the rover. The gray circles constitute the d-set for the influence source a_{sat} .

exact influence computation requires solving a large number of intractable inference problems. In fact, in most applications, the size of the d-set increases linearly in time, resulting in an exponentially increasing number of instantiations of the d-set. This means that representing an EIP takes exponential space, and computing (deducing) an EIP requires solving exponentially many and possibly hard inference problems. This motivates the idea of using *approximate influence point* (AIP) representations: we instead use advances in machine learning that allows us to generalize AIPs over d-separating sets. The overall idea consists of transforming the global model into a new approximate influence-augmented local model at which any solution method can be applied. Our method is therefore complementary to the planning method. The advantage lies in the reduction of the problem size and therefore in computational complexity.

The approach is straightforward but sketched in Algorithm 1 for completeness: first we collect samples of the local history D^t sufficient to predict the influence sources Y_{src}^t in the global model using an exploratory policy π_i^{Exp} for agent i (lines 1-3). In the second step, we learn the approximate influence point \hat{I}^t using the N trajectories of (D^t, Y_{src}^t) as training set (lines 4-5). Then, we construct the approximate local transitions \hat{T}_i using the learned influence point \hat{I} according to (1) (line 6). Then, we assume that the resulting local problem might be solved by simulation-based planning or RL approaches to derive a near optimal best-response $\hat{\pi}_i^*$ for agent i (line 7-9). The idea is that this phase uses $M \gg N$ episodes, thus making the initial cost of using the expensive global simulations negligible.

While planning with a learned approximate influence could lead to significant speed-ups, there is also a risk as the approximate influence point may induce inaccurate state transitions, leading to a loss in value. A key question therefore is: what constitutes good AIPs? What conditions need to hold on \hat{I} , for $\hat{\pi}_i^*$ to be close to optimal?

Algorithm 1 Exact Best Response to Approximate Influence

Require: exploratory policy π_i^{Exp} , policies π_{-i}

- 1: {Simulation:}
- 2: Create a dataset of N trajectories of the global model
- 3: Extract $(d_k^t, y_{\text{src},k}^t)_{k=1:N, t=1:h}$
- 4: {Train a Prediction Algorithm:}
- 5: Learn approximate influence \hat{I}^t from $(d_k^t, y_{\text{src},k}^t)_{k=1:N}$
- 6: Compute approximate local transitions $\hat{\mathcal{T}}_i$ from \hat{I}
- 7: {Solve the local planning/RL problem:}
- 8: Compute $\hat{\pi}_i^* = \text{MDPPlanner}(\hat{\mathcal{T}}_i)$
- 9: **return** $\hat{\pi}_i^*$

4 THEORETICAL LOSS BOUNDS

Here we want to provide guarantees on the value loss when using AIPs instead of EIPs to derive best-response policies. Such kind of results allow us to derive conditions for approximate influence to yield near-optimal solutions.

Formally, we consider two IALMs $\mathcal{M} = (\bar{\mathcal{S}}, A, \mathcal{T}, R, h, b^0)$ and $\hat{\mathcal{M}} = (\bar{\mathcal{S}}, A, \hat{\mathcal{T}}, R, h, b^0)$ sharing the same augmented state space, action space and rewards. They differ only in the transition functions \mathcal{T} and $\hat{\mathcal{T}}$ that are induced respectively by the EIP I and an AIP \hat{I} according to (1). We see $\hat{\mathcal{M}}$ as an approximation to \mathcal{M} . We omit the subscript i when referring to an IALM for agent i to ease the notation.

4.1 L^1 Loss Bound

We introduce first the necessary notation. We use \mathcal{V}_h^* to denote the objective optimal value for \mathcal{M} . $\hat{\pi}^*$ refers to the optimal policy in the approximate IALM $\hat{\mathcal{M}}$. $\mathcal{V}_h^{\hat{\pi}^*}$ denotes the value achieved by policy $\hat{\pi}^*$ in the IALM \mathcal{M} . Our aim is to bound the value loss given by the difference $\mathcal{V}_h^* - \mathcal{V}_h^{\hat{\pi}^*}$. We define $|R| \triangleq \max_{a,s} |R(s, a)|$. We use $\|\cdot\|_1$ and D_{KL} to denote the 1-norm and the KL divergence between probability distributions.

The proof of the value loss bound derived is divided into two steps. We proceed first by bounding the value loss with the difference between the IALM transitions functions $\|\mathcal{T} - \hat{\mathcal{T}}\|_1$. Then, we prove an upper bound for $\|\mathcal{T} - \hat{\mathcal{T}}\|_1$ in terms of the difference $\|I - \hat{I}\|_1$. Finally, combining these two results we derive an upper bound for the value loss in terms of the distance between the EIP and the AIP $\|I - \hat{I}\|_1$. We collect the proofs of all the following claims in the Appendix A.

Since the IALM $\hat{\mathcal{M}}$ is essentially an approximation of the exact influence IALM \mathcal{M} with imprecise transitions, we apply the loss bounds for MDPs with uncertain transition probabilities [15, 24, 39] to the case of the IALMs.

Theorem 1. Consider the two IALMs \mathcal{M} and $\hat{\mathcal{M}}$, the following loss bound holds:

$$\|\mathcal{V}_h^* - \mathcal{V}_h^{\hat{\pi}^*}\|_\infty \leq 2h^2|R| \max_t \max_{\bar{s}^t, a^t} \|(\mathcal{T}(\cdot|\bar{s}^t, a^t) - \hat{\mathcal{T}}(\cdot|\bar{s}^t, a^t))\|_1. \quad (2)$$

The importance is that we can bound the value loss when the IALM transition functions $\mathcal{T}, \hat{\mathcal{T}}$ induced by I, \hat{I} are sufficiently close.

For the second step, we use the relation between the IALM transitions \mathcal{T} and the influence point I expressed by (1).

Lemma 1. Consider the IALMs transitions \mathcal{T} and $\hat{\mathcal{T}}$. For any t , augmented state $\bar{s}^t = (x^t, d^t)$ and action a^t ,

$$\|(\mathcal{T}(\cdot|\bar{s}^t, a^t) - \hat{\mathcal{T}}(\cdot|\bar{s}^t, a^t))\|_1 \leq \|(I^t(\cdot|d^t) - \hat{I}^t(\cdot|d^t))\|_1. \quad (3)$$

Combining Theorem 1 and Lemma 1, we obtain the L^1 loss bound.

Theorem 2. Consider an IALM $\mathcal{M} = (\mathcal{S}, A, \mathcal{T}, R, h, b^0)$ and an AIP \hat{I} inducing $\hat{\mathcal{M}} = (\mathcal{S}, A, \hat{\mathcal{T}}, R, h, b^0)$. Then, a value loss bound in terms of the 1-norm error is given by

$$\|\mathcal{V}_h^* - \mathcal{V}_h^{\hat{\pi}^*}\|_\infty \leq 2h^2|R| \max_{t, d^t} \|(I^t(\cdot|d^t) - \hat{I}^t(\cdot|d^t))\|_1. \quad (4)$$

This shows that the value loss is bounded by the worst case L^1 -distance between the exact and the approximate influence over all the possible d-set instantiations.

4.2 KL Divergence Bound

We now present a loss bound in terms of the KL divergence between the approximate and the exact influence. Since the cross entropy and KL divergence differ solely by an additive constant, this result establishes a relation between the value loss and the cross entropy error for influence approximation.

Corollary 1. Consider an IALM $\mathcal{M} = (\mathcal{S}, A, \mathcal{T}, R, h, b^0)$ and an AIP \hat{I} inducing $\hat{\mathcal{M}} = (\mathcal{S}, A, \hat{\mathcal{T}}, R, h, b^0)$. Then, a value loss bound in terms of KL divergence error is given by

$$\|\mathcal{V}_h^* - \mathcal{V}_h^{\hat{\pi}^*}\|_\infty \leq 2h^2|R| \max_{t, d^t} \sqrt{2D_{KL}(I^t(\cdot|d^t) \parallel \hat{I}^t(\cdot|d^t))}. \quad (5)$$

We see that the performance loss can be bounded by the max KL divergence. Cross entropy loss optimizes the mean of such loss $\mathbb{E}_{t, D^t} [D_{KL}(I^t(\cdot|D^t) \parallel \hat{I}^t(\cdot|D^t))]$ and therefore is aligned with this bound: even though it does not optimize the max itself, it is intuitively clear that in many problems a low mean will imply a low max error, even the more since the mean is known to be sensitive to outliers. Moreover, this is an asymptotically tight bound. That is, when the KL divergence tends to zero the approximate influence solution approaches the true optimal one. This suggests that neural networks learning approaches are well suited for the approximate influence learning task and that the cross entropy, which has been widely used as test error, can give a priori insight on the value loss.

4.3 Probabilistic Loss Bound

The previous section gives an idea of what AIPs properties can guarantee bounded value loss. However, the direct application of Theorem 2 and Corollary 1 requires the distance to the true influence point I , which is unknown. In this section, we present an approach to overcome this limitation, by providing a probabilistic loss bound that depends only on the distance to an empirical influence distribution, which can be measured using a test set.

Precisely, assume that for a given instantiation d^t of the d-set at time t we have N samples of the influence sources $\{y_{\text{src},1}^t, \dots, y_{\text{src},N}^t\}$ and let

$$I_N^t(y_{\text{src}}^t | d^t) = \frac{1}{N} \sum_{k=1}^N \delta_{y_{\text{src},k}^t}(y_{\text{src}}^t),$$

denote the empirical conditional distribution. Our result presents a value loss bound in terms of the distance between the empirical influence I_N^t and the approximate \hat{I}^t .

Theorem 3. Consider an IALM $\mathcal{M} = (S, A, \mathcal{T}, R, h, b^0)$ and an AIP \hat{I} inducing $\hat{\mathcal{M}} = (S, A, \hat{\mathcal{T}}, R, h, b^0)$. Assume that for every time t and d-set instantiation d^t , we have at least a sample of size N of influence sources. Then for every $\varepsilon > 0$

$$\mathbb{P}\left(\|\mathcal{V}_h^* - \mathcal{V}_h^{\hat{\pi}^*}\|_\infty \leq 2h^2|R| \max_{t,d^t} \|(I_N^t(\cdot | d^t) - \hat{I}^t(\cdot | d^t)\|_1 + \varepsilon\right) \geq 1 - h|D^h|(2^{|Y_{\text{src}}|} - 2)e^{-N\frac{\varepsilon^2}{2}}, \quad (6)$$

where $|Y_{\text{src}}|$ is the cardinality of the influence sources space and $|D^h|$ the cardinality of the d-sets space at time h .

This theorem states that, with high probability, the value loss of using an AIP \hat{I} is upper bounded by the empirical error (that we can measure using a test set). We believe that this is a first step towards bounds that can be used in practical applications.

However, the bound in Theorem 3, still requires an intractable maximization over all possible instantiations of d-sets (and needs $N > \log(h|D^h|2^{|Y_{\text{src}}|})$ samples for each of these). Moreover, the maximization over d-sets might be too conservative in many cases. In this respect, identifying versions of these bounds that would work with expectations over d-sets, rather than maximization, is one of the important directions of future work that our paper identifies.

5 MULTIAGENT IMPLICATIONS

So far, we have focused on the perspective of a single agent, that computes a best response against the fixed policies of other agents. However, the results in this paper can have important implications also for settings where we optimize or solve for the policies of multiple agents at the same time. In fact, the insights of influence-based abstraction originated from the study of multiagent systems [3–5, 33, 38, 41, 42, 44, 45, 47–49], so these implications should hardly be surprising. Nevertheless, we think it is useful to spell out some of these implications and will do so in the remainder of this section.

First, we point out that the best response setting that we consider is very general. In fact, the notion of a ‘fixed policy’ of an agent in a POSG is very powerful: such a fixed policy is a mapping from histories of actions and observations to distributions over actions and therefore powerful enough to model learning agents. This means that the fixed policies that we compute a best response against could include, e.g., a Q-learning agent.

A second implication is for the computation of equilibria in POSGs. Many methods for computing Nash equilibria in POSGs [6, 11, 21, 25, 32], use best-response computation as an inner loop. In many cases, such as in the double-oracle algorithm [25] or the parallel Nash Memory [32], replacing such a best-response computation with an ϵ -best response computation can enable us to

compute ϵ -approximate Nash Equilibria (ϵ -NEs) [28], in which no player can benefit more than ϵ from deviating. As such, our results that show under what conditions on the influence predictions, we can compute a best-response, may lead to computationally feasible paths to compute ϵ -NEs.

Even in cases where computing ϵ -NEs will remain out of reach, our results can provide insight in complex MAS.

Observation 1. Given a method E to estimate an AIP with an error (maximum L_1 norm) of at most ϵ_1 , we can verify if a particular joint policy $\pi = (\pi_1, \dots, \pi_n)$ is an $(2h^2|R|\epsilon_1)$ -NE as follows: 1) use E to estimate the influence \hat{I}_i on each agent i 2) verifying if π_i is an optimal solution in the IALM constructed for agent i .

Of course, the question of how to develop such estimators E is not trivial in the general case, but there are many special cases with compact influence descriptions where this is possible [12, 34].

Moreover, IBA serves as the basis for *influence search* [4, 45, 48] in cooperative settings. The key idea is that an influence point captures all the relevant information about many different policies of the other agents. That is, different joint policies might induce the same influences on the local models of the agents. Thus, the space of ‘joint influence points’ $I = (I_1, \dots, I_n)$ can be much smaller than the space of joint policies $\pi = (\pi_1, \dots, \pi_n)$, and it can be much more efficient to search through the former. [49].¹ Nevertheless, the space of joint influence points I can still be prohibitively large, and Witwicki [46] (chapter 7) developed an approximate version where the generated influences are separated by some minimum distance ϵ . He showed that the empirical value loss of such an approach is bounded. Our Theorem 2 gives theoretical support for this:

Observation 2. The value loss of the approximate influence search procedures, such as those by Witwicki [46], can be bounded using Theorem 2.²

Our goal here is not to directly give this quantitative result. In fact, in this work we have targeted the general setting of factored POSGs, while influence search methods have so far only been defined for strict subclasses (and using slightly different definitions of influence). However, this observation makes clear how our bounds can be used to inform future algorithms.

6 EMPIRICAL EVALUATION

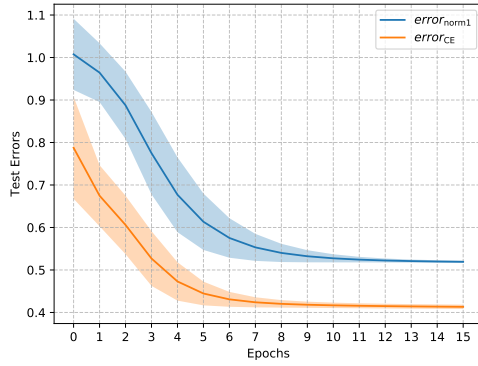
The bounds presented in Section 4 establish a relation between the value loss and the cross entropy of the influence approximations. In particular, they suggest that the *mean* cross entropy loss is aligned with the objective of minimizing the performance loss.

Here we evaluate if this alignment translates into practical settings by investigating the relation between the mean cross entropy

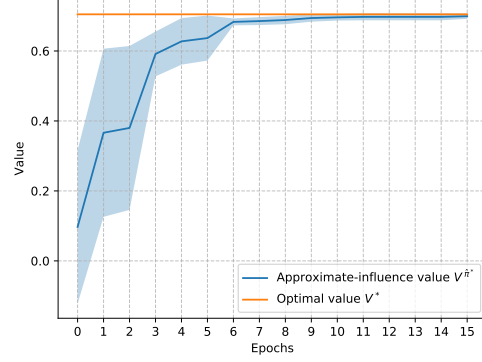
$$\text{CE}(I, \hat{I}) \triangleq \mathbb{E}_{t,D^t} [\text{CE}(I^t(\cdot | D^t), \hat{I}^t(\cdot | D^t))]$$

¹Roughly speaking, an influence search algorithm searches in the space of possible joint influences, and for each joint influence point $I = (I_1, \dots, I_n)$, it solves a local constrained best-response problem for each agent (possibly in parallel): each agent i computes a best-response $\hat{\pi}^*(I)$ to I_i constrained to inducing influences I_{-i} on the local models of the other agents.

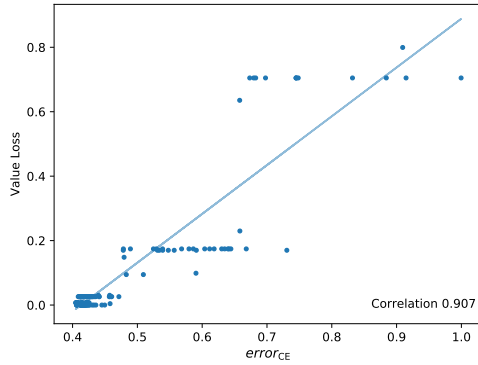
²Note, we can not directly plug Witwicki’s minimum distance parameter ϵ into our Theorem 2 to provide a quantitative result. This is due to technical difference between the definition of influence in that work and the more general influence definition used by influence-base abstraction.



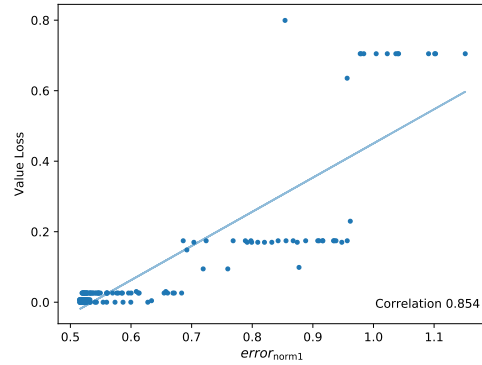
(a) Test errors for increasing training epochs.



(b) Value achieved by $\hat{\pi}^*$ compared to the optimal value for increasing training epochs.



(c) Correlation between value loss and $error_{CE}$.



(d) Correlation between value loss and $error_{norm1}$.

Figure 3: Planetary Exploration.

and the performance loss $\mathcal{V}_h^* - \mathcal{V}_h^{\hat{\pi}^*}$. Namely, we expect to see that a better influence approximation in terms of cross entropy loss, indeed, leads to a smaller value loss. Here we try to validate this hypothesis.

Similarly, we investigate to what extent the *mean* 1-norm error

$$\|I - \hat{I}\|_1 \triangleq \mathbb{E}_{t, D^t} [\|I^t(\cdot|D^t) - \hat{I}^t(\cdot|D^t)\|_1]$$

allows to a priori assess the quality of the approximations in terms of the value loss. In fact, according to the results in Section 4, the 1-norm has the potential to provide a tighter bound for the performance loss. If experimentally confirmed, this would motivate future work to investigate the possibility to use different training losses based on L^1 distance.

6.1 Experimental setup

We follow the procedure sketched in Algorithm 1. That is, we first run the simulations from the global model using an exploratory random policy π^{Exp} for the local agent and the set of fixed policies for the other agents. We collect the samples of influence sources and d-sets $\{y_{\text{src},k}^t, d_k^t\}_{t=1:h,k=1:N}$. We train a LSTM neural network with

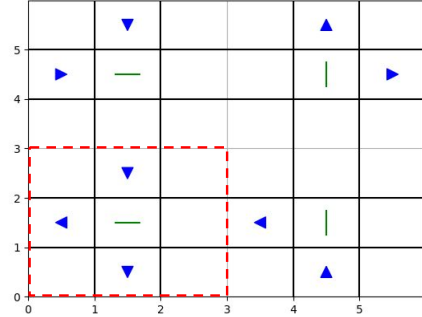
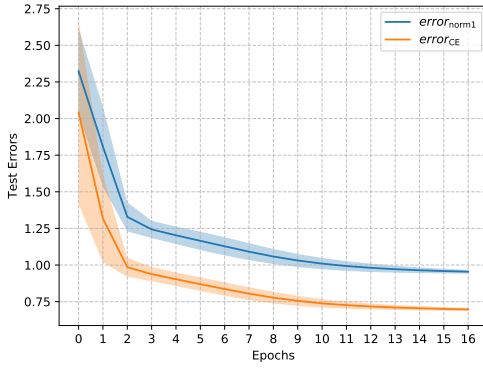
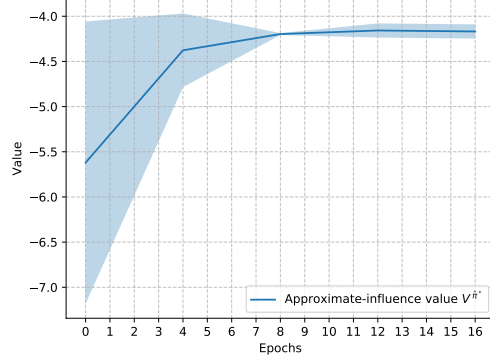


Figure 4: Traffic network. The local model is delimited by the dotted square. The blue triangles represent the vehicles and the green bars the traffic lights.

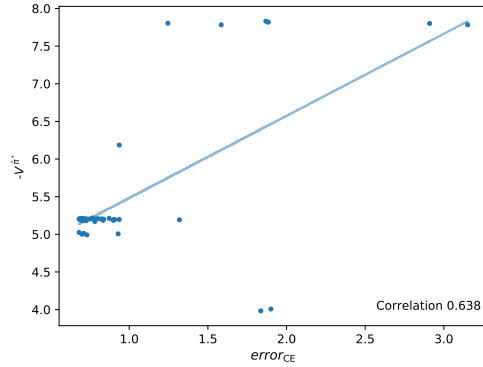
cross entropy loss to induce the approximate influence $\hat{I}^t(\cdot|D^t)$. At different training epochs, for the corresponding approximations of the influence, we build the approximate-influence local model. Then, we compute the optimal policy $\hat{\pi}^*$ in the approximate-influence model through value iteration [8]. We evaluate the policy $\hat{\pi}^*$ in the



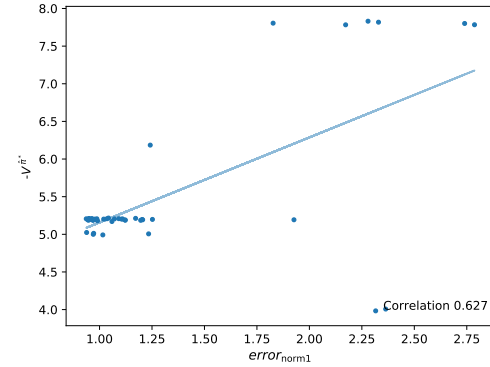
(a) Test errors for increasing training epochs.



(b) Value achieved by $\hat{\pi}^*$ for increasing training epochs computed every 4 epochs.



(c) Correlation between value loss and $error_{CE}$.



(d) Correlation between value loss and $error_{norm1}$.

Figure 5: Traffic network.

global model using M simulations to obtain the value achieved $\mathcal{V}_h^{\hat{\pi}^*}$. Note that since we use an exact solution method to compute the policy $\hat{\pi}^*$ in the approximate-influence model, any other solution method would get lower performance in the local model. For each epoch, to assess the quality of the approximation, we use Monte Carlo estimators for the mean cross entropy $CE(I, \hat{I})$ and the 1-norm error $\|I - \hat{I}\|_1$, computed using a test set as

$$\begin{aligned} error_{CE} &= -\frac{1}{h} \sum_{t=1}^h \frac{1}{N} \sum_{k=0}^N \ln \left(\hat{I}^t(y_{src,k}^t | d_k^t) \right), \\ error_{norm1} &= \frac{1}{h} \sum_{t=1}^h \frac{1}{N} \sum_{k=0}^N \left\| \delta_{y_{src,k}^t}(\cdot) - \hat{I}^t(\cdot | d_k^t) \right\|_1, \end{aligned} \quad (7)$$

We compute the average and standard deviation of the $error_{CE}$ and $error_{norm1}$ over different iterations of the same experiment. For any iteration, we repeat entirely the steps described above: we recollect training and testing samples from the global model, retrain the neural network etc. When the problem is sufficiently easy to solve, we compute the optimal value \mathcal{V}_h^* and then we measure the correlation between $error_{CE}$, $error_{norm1}$ and the value loss

$\mathcal{V}_h^* - \mathcal{V}_h^{\hat{\pi}^*}$. Otherwise, we measure the correlation between the test errors and $-\mathcal{V}_h^{\hat{\pi}^*}$. In fact, since the optimal value \mathcal{V}_h^* is constant for increasing epochs, it does not affect the correlation. That is, $Corr(error, \mathcal{V}_h^* - \mathcal{V}_h^{\hat{\pi}^*}) = Corr(error, -\mathcal{V}_h^{\hat{\pi}^*})$.

We run the experiments in three domains: a version of the planetary exploration [48], a traffic domain and the fire fighters problem [29]. Section 2.3 provides the overview of the planetary exploration domain and high level descriptions of the other domains follow. For details of all domains, please see the Appendix B.

6.1.1 Traffic Network. In this domain, we simulate a traffic network with 4 intersections (see Figure 4). The sensors of the traffic lights at each intersection provide information on the 3×3 local grid around them. In Figure 4, the dotted red square represents the local model for the protagonist agent. The other traffic lights employ hand-coded policies prioritizing fixed lanes. The goal of the agent is to minimize the total number of vehicles waiting at the local intersection. In order to act optimally, the local agent only needs to predict if there will be incoming cars from the *east* and *north* lanes of the local model the next time step. The outgoing cars have some probability to re-enter in the network from other lanes. That is, the outgoing vehicles from *south* and *west* can affect the decisions of

other traffic lights and consequently, the vehicles inflow in the local model at future time steps.

6.1.2 Fire fighters. We model a team of 2 agents that need to cooperate to extinguish fires in a row of 3 houses. At every time step, every agent can choose to fight fires at one of its 2 neighboring houses. The goal of each agent is to minimize the number of neighboring houses that are burning. We take the perspective of one agent with a local model including only the two neighboring houses.

6.2 Experimental results

Figures 3(a), 5(a), 6(a) show the test errors measured by $error_{CE}$ and $error_{norm1}$ (7), as functions of the training epochs for the three domains. They show that performance in terms of cross entropy and 1-norm test errors improves monotonically with the number of epochs. These trends suggest that the AIP improves with training, the question is if this also corresponds to a value loss decrease. Looking at Figure 3(b) this seems to be the case in the planetary exploration setting. We see that the performance of the policy derived from the approximate-influence IALM is very close to optimal from 6 epochs onward, right about when the training of the neural network starts to stagnate. Moreover, Figure 3(c) and 3(d) show that the decrease in mean empirical cross entropy or 1-norm error indeed correlates well with actual value loss. In the traffic domain, we also see that there is a significant improvement in the value achieved by the approximate-influence policy $\hat{\pi}^*$ for increasing number of epochs in Figure 5(b). The test errors seem still well aligned with the value loss in Figures 5(c), 5(d). For the fire fighters domain, Figure 6(b) shows that the value improves over training epochs coherently with the decrease of the test errors.

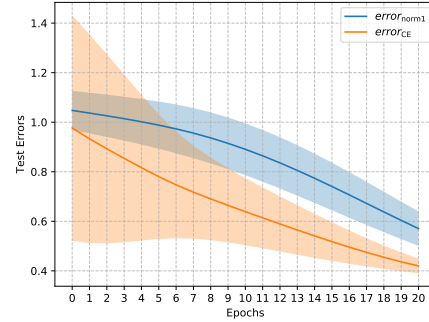
For more results on correlation analysis on different settings of the planetary exploration, see the Appendix C.

We can conclude that both the empirical cross entropy error and the 1-norm errors correlate well with the value loss and therefore provide a priori insight on the quality of the influence-approximation in terms of the value achieved.

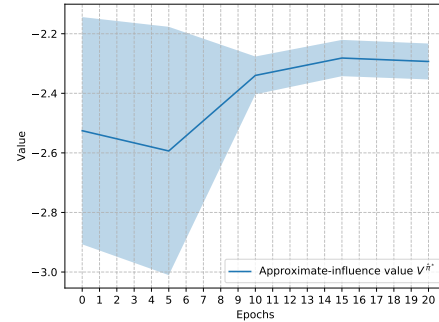
7 RELATED WORK

Existing methods to compute best responses against other agents fixed policies [27, 31, 36] involve reasoning over the entire state space and other agents action-observation histories. Precisely, in order to compute a best response, an agent has to maintain a belief over the full state and action-observation histories of other agents. However, the state space can be large and the number of histories increases exponentially in time. Therefore, these approaches are not effective for large state spaces and multiple agents systems. By modeling the effects of the non-local part of the system, influence-based abstraction allows to reason only over limited number of state variables included in the local model.

Abstraction has been widely studied as a technique to accelerate learning and improve scalability in complex (multiagent) problems. It allows to extract relevant features of the dynamics and provide compact representations of this information. Many abstraction approaches have been suggested [2, 14, 16, 23, 37] but they all share a common limitation: in order to guarantee bounded loss, the resulting abstract states (which are clusters of ground states)



(a) Test errors for increasing training epochs.



(b) Value achieved by $\hat{\pi}^*$ for increasing training epochs computed every 5 epochs.

Figure 6: Fire Fighters Problem.

must have similar transition probabilities for all ground states they represent. However, when we want to abstract away entire sets of state variables such guarantees will typically not be possible. Influence-based abstraction enables abstracting away factors still providing guarantees of optimality even though the aggregated states have very different transition probabilities.

8 CONCLUSIONS AND DISCUSSION

In this paper, we provided a priori quality guarantees for the value loss resulting from approximating the influence point. Our results show that the objective of a neural network trained with the cross entropy loss is well aligned with the goal of minimizing the value loss. Our empirical results demonstrate that empirical (mean) estimators of the cross entropy and the 1-norm are predictive of the value loss. We used this insight to evaluate the transfer of our theoretical results to practical scenarios.

The current formulation of the loss bounds, however, involves a maximization over the space of all the possible instantiations of the d-set, which might grow exponentially in time. In future work, we would like to derive expressions that do not need a maximization, but for example are in expectation over a sampling process. This would lead to tighter bounds, which could be used in practice for model selection or value loss estimation.

9 ACKNOWLEDGEMENTS

This project had received funding from the European Research Council (ERC) under the European Union’s Horizon 2020 research and innovation programme (grant agreement No.758824 –INFLU-ENCE).



REFERENCES

- [1] D. Bahdanau, P. Brakel, K. Xu, A. Goyal, R. Lowe, J. Pineau, A. C. Courville, and Y. Bengio. An actor-critic algorithm for sequence prediction. In *International Conference on Learning Representations (ICLR)*, pages 24–26, 2017.
- [2] A. Bai, S. Srivastava, and S. J. Russell. Markovian state and action abstractions for MDPs via hierarchical MCTS. In *International Joint Conference on Artificial Intelligence (IJCAI)*, pages 3029–3039, 2016.
- [3] R. Becker, S. Zilberstein, and V. Lesser. Decentralized markov decision processes with event-driven interactions. In *International Conference on Autonomous Agents and Multiagent Systems (AAMAS)*, pages 302–309, 2004.
- [4] R. Becker, S. Zilberstein, V. Lesser, and C. V. Goldman. Transition-independent decentralized Markov decision processes. In *International Conference on Autonomous Agents and Multiagent Systems (AAMAS)*, pages 41–48, 2003.
- [5] R. Becker, S. Zilberstein, V. Lesser, and C. V. Goldman. Solving transition independent decentralized markov decision processes. *Journal of Artificial Intelligence Research*, 22:423–455, 2004.
- [6] U. Berger. Brown’s original fictitious play. *Journal of Economic Theory*, 135(1):572–578, 2007.
- [7] D. S. Bernstein, R. Givan, N. Immerman, and S. Zilberstein. The complexity of decentralized control of Markov decision processes. *Mathematics of Operations Research*, 27(4):819–840, 2002.
- [8] D. P. Bertsekas. *Dynamic programming and optimal control*. Athena scientific, 1995.
- [9] C. M. Bishop. *Pattern recognition and machine learning*. Springer, 2006.
- [10] C. Boutilier, T. Dean, and S. Hanks. Decision-theoretic planning: structural assumptions and computational leverage. *Journal of Artificial Intelligence Research*, 11:1–94, 1999.
- [11] G. W. Brown. Iterative solution of games by fictitious play. *Activity analysis of production and allocation*, 13(1):374–376, 1951.
- [12] R. Chitnis and T. Lozano-Pérez. Learning compact models for planning with exogenous processes. pages 813–822, 2020.
- [13] T. M. Cover and J. A. Thomas. *Elements of information theory*. John Wiley & Sons, 2012.
- [14] R. Dearden and C. Boutilier. Abstraction and approximate decision-theoretic planning. *Artificial Intelligence*, 89(1-2):219–283, 1997.
- [15] K. V. Delgado, S. Sanner, and L. N. De Barros. Efficient solutions to factored MDPs with imprecise transition probabilities. *Artificial Intelligence*, 175(9-10):1498–1527, 2011.
- [16] R. Givan, S. Leach, and T. Dean. Bounded-parameter markov decision processes. *Artificial Intelligence*, 122(1-2):71–109, 2000.
- [17] C. V. Goldman and S. Zilberstein. Decentralized control of cooperative systems: Categorization and complexity analysis. *Journal of Artificial Intelligence Research*, 22:143–174, 2004.
- [18] E. A. Hansen, D. S. Bernstein, and S. Zilberstein. Dynamic programming for partially observable stochastic games. In *AAAI Conference on Artificial Intelligence*, pages 709–715, 2004.
- [19] S. Hochreiter and J. Schmidhuber. Long short-term memory. *Neural Computation*, 9(8):1735–1780, 1997.
- [20] F. Karim, S. Majumdar, H. Darabi, and S. Chen. LSTM fully convolutional networks for time series classification. *IEEE*, 6:1662–1669, 2017.
- [21] M. Lanctot, V. Zambaldi, A. Gruslys, A. Lazaridou, J. Perolat, D. Silver, and T. Graepel. A unified game-theoretic approach to multiagent reinforcement learning. In *Advances in Neural Information Processing Systems (NIPS)*, 2017.
- [22] C. Lea, M. D. Flynn, R. Vidal, A. Reiter, and G. D. Hager. Temporal convolutional networks for action segmentation and detection. In *IEEE Conference on Computer Vision and Pattern Recognition*, pages 156–165, 2017.
- [23] L. Li, T. J. Walsh, and M. L. Littman. Towards a unified theory of state abstraction for MDPs. In *International Symposium on Artificial Intelligence and Mathematics (ISAIM)*, pages 531–539, 2006.
- [24] A. Mastin and P. Jaillet. Loss bounds for uncertain transition probabilities in Markov decision processes. In *IEEE Conference on Decision and Control*, pages 6708–6715, 2012.
- [25] H. B. McMahan, G. J. Gordon, and A. Blum. Planning in the presence of cost functions controlled by an adversary. In *International Conference on Machine Learning (ICML)*, pages 536–543, 2003.
- [26] K. P. Murphy and S. Russell. *Dynamic Bayesian Networks: Representation, Inference and Learning*. PhD thesis, 2002.
- [27] R. Nair, M. Tambe, M. Yokoo, D. V. Pynadath, and S. Marsella. Taming decentralized POMDPs: Towards efficient policy computation for multiagent settings. In *International Joint Conference on Artificial Intelligence (IJCAI)*, pages 705–711, 2003.
- [28] N. Nisan, T. Roughgarden, E. Tardos, and V. V. Vazirani. *Algorithmic Game Theory*. Cambridge University Press, 2007.
- [29] F. A. Oliehoek. *Value-based planning for teams of agents in stochastic partially observable environments*. Amsterdam University Press, 2010.
- [30] F. A. Oliehoek and C. Amato. *A Concise Introduction to Decentralized POMDPs*.
- [31] F. A. Oliehoek and C. Amato. Best response Bayesian reinforcement learning for multiagent systems with state uncertainty. In *AAMAS Workshop on Multiagent Sequential Decision Making Under Uncertainty*, 2014.
- [32] F. A. Oliehoek, E. D. De Jong, and N. Vlassis. The parallel nash memory for asymmetric games. In *Genetic and Evolutionary Computation Conference*, pages 337–344, 2006.
- [33] F. A. Oliehoek, M. T. J. Spaan, and S. Witwicki. Factored upper bounds for multiagent planning problems under uncertainty with non-factored value functions. In *International Joint Conference on Artificial Intelligence (IJCAI)*, pages 1645–1651, July 2015.
- [34] F. A. Oliehoek, S. Witwicki, and L. P. Kaelbling. A sufficient statistic for influence in structured multiagent environments. *arXiv preprint arXiv:1907.09278*, 2019.
- [35] F. A. Oliehoek, S. J. Witwicki, and L. P. Kaelbling. Influence-based abstraction for multiagent systems. In *AAAI Conference on Artificial Intelligence*, 2012.
- [36] A. Panella and P. Gmytrasiewicz. Interactive pomdps with finite-state models of other agents. *Journal of Autonomous Agents and Multi-Agent Systems*, 31(4):861–904, 2017.
- [37] M. Petrik and D. Subramanian. Raam: The benefits of robustness in approximating aggregated MDPs in reinforcement learning. In *Advances in Neural Information Processing Systems (NIPS)*, pages 1979–1987, 2014.
- [38] M. Petrik and S. Zilberstein. A bilinear programming approach for multiagent planning. *Journal of Artificial Intelligence Research*, 35(1):235–274, 2009.
- [39] A. L. Strehl, L. Li, and M. L. Littman. Reinforcement learning in finite MDPs: Pac analysis. *Journal of Machine Learning Research*, 10(9):2413–2444, 2009.
- [40] P. Varakantham, J.-y. Kwak, M. E. Taylor, J. Marecki, P. Scerri, and M. Tambe. Exploiting coordination locales in distributed pomdps via social model shaping. In *International Conference on Automated Planning and Scheduling (ICAPS)*, 2009.
- [41] P. Varakantham, J.-y. Kwak, M. E. Taylor, J. Marecki, P. Scerri, and M. Tambe. Exploiting coordination locales in distributed POMDPs via social model shaping. In *International Conference on Automated Planning and Scheduling (ICAPS)*, 2009.
- [42] P. Velagapudi, P. Varakantham, P. Scerri, and K. Sycara. Distributed model shaping for scaling to decentralized POMDPs with hundreds of agents. In *International Conference on Autonomous Agents and Multiagent Systems (AAMAS)*, 2011.
- [43] T. Weissman, E. Ordentlich, G. Seroussi, S. Verdú, and M. J. Weinberger. Inequalities for the L1 deviation of the empirical distribution. Technical report, 2003.
- [44] S. Witwicki and E. Durfee. From policies to influences: A framework for nonlocal abstraction in transition-dependent Dec-POMDP agents. In *International Conference on Autonomous Agents and Multiagent Systems (AAMAS)*, pages 1397–1398, 2010.
- [45] S. Witwicki, F. A. Oliehoek, and L. P. Kaelbling. Heuristic search of multiagent influence space. In *International Conference on Autonomous Agents and Multiagent Systems (AAMAS)*, pages 973–981, June 2012.
- [46] S. J. Witwicki. *Abstracting Influences for Efficient Multiagent Coordination Under Uncertainty*. PhD thesis, University of Michigan, 2011.
- [47] S. J. Witwicki and E. H. Durfee. Flexible approximation of structured interactions in decentralized Markov decision processes. In *International Conference on Autonomous Agents and Multiagent Systems (AAMAS)*, pages 1251–1252, 2009.
- [48] S. J. Witwicki and E. H. Durfee. Influence-based policy abstraction for weakly-coupled dec-POMDPs. In *International Conference on Automated Planning and Scheduling (ICAPS)*, 2010.
- [49] S. J. Witwicki and E. H. Durfee. Towards a unifying characterization for quantifying weak coupling in Dec-POMDPs. In *International Conference on Autonomous Agents and Multiagent Systems (AAMAS)*, pages 29–36, Taipei, Taiwan, 2011.

A THEORETICAL LOSS BOUNDS PROOFS

Here we collect all the proofs for the claims in Section 4. We use the notation introduced in Section 4.

Theorem 1. Consider the two IALMs \mathcal{M} and $\hat{\mathcal{M}}$, the following loss bound holds:

$$\|\mathcal{V}_h^* - \mathcal{V}_h^{\hat{\pi}^*}\|_\infty \leq 2h^2|R| \max_t \max_{\bar{s}^t, a^t} \|(\mathcal{T}(\cdot | \bar{s}^t, a^t) - \hat{\mathcal{T}}(\cdot | \bar{s}^t, a^t))\|_1.$$

PROOF. We apply Corollary 2 [24] to the case of uncertainty in transition probabilities for IALMs. More precisely, Corollary 2 states that given a finite-horizon MDP $M = (S, A, R, T, h)$ and an approximate MDP with uncertain transitions $\hat{M} = (S, A, R, \hat{T}, h)$, the performance loss when using the optimal policy $\hat{\pi}^*$ for the approximate transition model \hat{M} in the true model M is bounded by

$$\|V_h^* - V_h^{\hat{\pi}^*}\|_\infty \leq 2h^2|R| \max_{s,a} \|T(\cdot | s, a) - \hat{T}(\cdot | s, a)\|_1.$$

To apply this result in the context of the IALMs \mathcal{M} and $\hat{\mathcal{M}}$, we only need to add a maximization over the time steps since the d-sets (accordingly the state space and transition functions) evolves over time. \square

Lemma 1. Consider the IALMs transitions \mathcal{T} and $\hat{\mathcal{T}}$. For any t , augmented state $\bar{s}^t = (x_{\text{int}}^t, x_{\text{dest}}^t, d^t)$ and action a^t ,

$$\|(\mathcal{T}(\cdot | \bar{s}^t, a^t) - \hat{\mathcal{T}}(\cdot | \bar{s}^t, a^t))\|_1 \leq \|(I^t(\cdot | d^t) - \hat{I}^t(\cdot | d^t))\|_1.$$

PROOF. According to the expression for the IALM transitions (equation (1) in the paper),

$$\begin{aligned} |\mathcal{T}(\bar{s}^{t+1} | \bar{s}^t, a^t) - \hat{\mathcal{T}}(\bar{s}^{t+1} | \bar{s}^t, a^t)| &= T(x_{\text{int}}^{t+1} | x^t, a^t) \left| \sum_{y_{\text{src}}^t} T(x_{\text{dest}}^{t+1} | x^t, y_{\text{src}}^t, a^t) [I^t(y_{\text{src}}^t | d^t) - \hat{I}^t(y_{\text{src}}^t | d^t)] \right| \\ &\leq T(x_{\text{int}}^{t+1} | x^t, a^t) \sum_{y_{\text{src}}^t} T(x_{\text{dest}}^{t+1} | x^t, y_{\text{src}}^t, a^t) |I^t(y_{\text{src}}^t | d^t) - \hat{I}^t(y_{\text{src}}^t | d^t)|. \end{aligned}$$

Therefore,

$$\begin{aligned} \|(\mathcal{T}(\cdot | \bar{s}^t, a^t) - \hat{\mathcal{T}}(\cdot | \bar{s}^t, a^t))\|_1 &= \sum_{\bar{s}^{t+1}} |\mathcal{T}(\bar{s}^{t+1} | \bar{s}^t, a^t) - \hat{\mathcal{T}}(\bar{s}^{t+1} | \bar{s}^t, a^t)| \\ &\leq \sum_{x_{\text{int}}^{t+1}, x_{\text{dest}}^{t+1}} T(x_{\text{int}}^{t+1} | x^t, a^t) \sum_{y_{\text{src}}^t} T(x_{\text{dest}}^{t+1} | x^t, y_{\text{src}}^t, a^t) |I^t(y_{\text{src}}^t | d^t) - \hat{I}^t(y_{\text{src}}^t | d^t)| \\ &= \sum_{y_{\text{src}}^t} |I^t(y_{\text{src}}^t | d^t) - \hat{I}^t(y_{\text{src}}^t | d^t)| \sum_{x_{\text{int}}^{t+1}} T(x_{\text{int}}^{t+1} | x^t, a^t) \sum_{x_{\text{dest}}^{t+1}} T(x_{\text{dest}}^{t+1} | x^t, y_{\text{src}}^t, a^t) \\ &= \sum_{y_{\text{src}}^t} |I^t(y_{\text{src}}^t | d^t) - \hat{I}^t(y_{\text{src}}^t | d^t)| \\ &= \|I^t(\cdot | d^t) - \hat{I}^t(\cdot | d^t)\|_1. \end{aligned} \quad \square$$

Theorem 2. Consider an IALM $\mathcal{M} = (S, A, \mathcal{T}, R, h, b^0)$ and an AIP \hat{I} inducing $\hat{\mathcal{M}} = (S, A, \hat{\mathcal{T}}, R, h, b^0)$. Then, a value loss bound in terms of the 1-norm error is given by

$$\|\mathcal{V}_h^* - \mathcal{V}_h^{\hat{\pi}^*}\|_\infty \leq 2h^2|R| \max_{t, d^t} \|(I^t(\cdot | d^t) - \hat{I}^t(\cdot | d^t))\|_1.$$

PROOF. It suffices to apply consecutively Theorem 1 and Theorem 1 to derive

$$\|\mathcal{V}_h^* - \mathcal{V}_h^{\hat{\pi}^*}\|_\infty \leq 2h^2|R| \max_t \max_{\bar{s}^t, a^t} \|(\mathcal{T}(\cdot | \bar{s}^t, a^t) - \hat{\mathcal{T}}(\cdot | \bar{s}^t, a^t))\|_1 \leq 2h^2|R| \max_t \max_{d^t} \|(I^t(\cdot | d^t) - \hat{I}^t(\cdot | d^t))\|_1. \quad \square$$

Corollary 1. Consider a IALM $\mathcal{M} = (S, A, \mathcal{T}, R, h, b^0)$ and an AIP \hat{I} inducing $\hat{\mathcal{M}} = (S, A, \hat{\mathcal{T}}, R, h, b^0)$. Then, a value loss bound in terms of KL divergence error is given by

$$\|\mathcal{V}_h^* - \mathcal{V}_h^{\hat{\pi}^*}\|_\infty \leq 2h^2|R| \max_{t, d^t} \sqrt{2D_{KL}(I^t(\cdot | d^t) \| \hat{I}^t(\cdot | d^t))}.$$

PROOF. It suffices to apply Pinsker inequality [13] to equation (4) to obtain the claim

$$\|\mathcal{V}_h^* - \mathcal{V}_h^{\hat{\pi}^*}\|_\infty \leq 2h^2|R| \max_{t, d^t} \|(I^t(\cdot | d^t) - \hat{I}^t(\cdot | d^t))\|_1 \leq 2h^2|R| \max_{t, d^t} \sqrt{2D_{KL}(I^t(\cdot | d^t) \| \hat{I}^t(\cdot | d^t))}. \quad \square$$

Before moving to the proof of Theorem 3, we first introduce this Lemma from [43].

Lemma 2. [43] Let p be a probability distribution over S and p_N the empirical distribution drawn from a sample of size N . For every $\varepsilon > 0$

$$\mathbb{P}(\|p - p_N\|_1 \geq \varepsilon) \leq (2^{|S|} - 2)e^{-N\frac{\varepsilon^2}{2}}.$$

Now we can move to the proof of Theorem 3.

Theorem 3. Consider a IALM $\mathcal{M} = (S, A, \mathcal{T}, R, h, b^0)$ and an AIP \hat{I} inducing $\hat{\mathcal{M}} = (S, A, \hat{\mathcal{T}}, R, h, b^0)$. Assume that for every time t and d-set instantiation d^t , we have at least an influence sources sample of size N . Then for every $\varepsilon > 0$

$$\mathbb{P}\left(\|\mathcal{V}_h^* - \mathcal{V}_h^{\hat{I}^*}\|_\infty \leq 2h^2|R| \max_{t,d^t} \|(I_N^t(\cdot|d^t) - \hat{I}^t(\cdot|d^t))\|_1 + \varepsilon\right) \geq 1 - h|D^h|(2^{|Y_{\text{src}}|} - 2)e^{-N\frac{\varepsilon^2}{2}},$$

where $|Y_{\text{src}}|$ is the cardinality of the influence sources space and $|D^h|$ the cardinality of the h step d-sets space.

PROOF. We apply Lemma 2 from [43] to the exact influence I^t and the empirical influence I_N^t , thereby obtaining

$$\mathbb{P}(\|I^t(\cdot|d^t) - I_N^t(\cdot|d^t)\|_1 \geq \varepsilon) \leq (2^{|Y_{\text{src}}|} - 2)e^{N\frac{\varepsilon^2}{2}},$$

where $|Y_{\text{src}}|$ refers to the cardinality of the space of the influence sources. Using the above inequality and the reverse triangle inequality

$$\|I^t(\cdot|d^t) - \hat{I}^t(\cdot|d^t)\|_1 - \|\hat{I}^t(\cdot|d^t) - I_N^t(\cdot|d^t)\|_1 \leq \|I^t(\cdot|d^t) - I_N^t(\cdot|d^t)\|_1,$$

we obtain

$$\begin{aligned} \mathbb{P}\left(\|I^t(\cdot|d^t) - \hat{I}^t(\cdot|d^t)\|_1 \geq \|\hat{I}^t(\cdot|d^t) - I_N^t(\cdot|d^t)\|_1 + \varepsilon\right) &\leq \mathbb{P}\left(\|I^t(\cdot|d^t) - \hat{I}^t(\cdot|d^t)\|_1 - \|\hat{I}^t(\cdot|d^t) - I_N^t(\cdot|d^t)\|_1 \geq \varepsilon\right) \\ &\leq \mathbb{P}(\|I^t(\cdot|d^t) - I_N^t(\cdot|d^t)\|_1 \geq \varepsilon) \leq (2^{|Y_{\text{src}}|} - 2)e^{N\frac{\varepsilon^2}{2}}. \end{aligned}$$

Thus by the union bound, we derive

$$\begin{aligned} &\mathbb{P}\left(\max_{t,d^t} \|I^t(\cdot|d^t) - \hat{I}^t(\cdot|d^t)\|_1 \leq \max_{t,d^t} \|I_N^t(\cdot|d^t) - \hat{I}^t(\cdot|d^t)\|_1 + \varepsilon\right) \\ &\geq \mathbb{P}\left(\bigcap_{t,d^t} \{\|I^t(\cdot|d^t) - \hat{I}^t(\cdot|d^t)\|_1 \leq \|I_N^t(\cdot|d^t) - \hat{I}^t(\cdot|d^t)\|_1 + \varepsilon\}\right) \\ &= 1 - \mathbb{P}\left(\bigcup_{t,d^t} \{\|I^t(\cdot|d^t) - \hat{I}^t(\cdot|d^t)\|_1 \geq \|I_N^t(\cdot|d^t) - \hat{I}^t(\cdot|d^t)\|_1 + \varepsilon\}\right) \\ &\geq 1 - \sum_{t,d^t} \mathbb{P}\left(\|I^t(\cdot|d^t) - \hat{I}^t(\cdot|d^t)\|_1 \geq \|I_N^t(\cdot|d^t) - \hat{I}^t(\cdot|d^t)\|_1 + \varepsilon\right) \\ &\geq 1 - \sum_{t,d^t} (2^{|Y_{\text{src}}|} - 2)e^{-N\frac{\varepsilon^2}{2}} \geq 1 - h|D^h|(2^{|Y_{\text{src}}|} - 2)e^{-N\frac{\varepsilon^2}{2}}. \end{aligned} \tag{8}$$

Now combining Theorem 2 and (8), we get the statement. \square

B EXPERIMENTAL SETUP

Here we describe the experimental setup for the domains we consider in Section 5.

B.1 Planetary Exploratory

The setting is a version of Planetary Exploration [48], in which a planetary rover has to explore an area. At the same time a second agent, a satellite, may help the rover by planning a route, which gives a higher probability of a successful move of the rover. Figure 1 in the paper shows a depiction of the three time steps dynamic Bayesian network [26]. If the rover fails to move it receives a penalty of -0.5 and reaching the target position results in a reward of 10. The satellite action of helping or not helping is denoted by $a_{\text{sat}} \in \{0, 1\}$, while the (non)-availability of a routing plan is a binary factor $pl \in \{\text{plan}, \neg\text{plan}\}$. The action a_{sat} of the satellite depends on its own charge status, a resource which it has to manage as well. In the result presented in the paper, the satellite will employ a stochastic policy such that whenever the level of the battery is lower than a given threshold, it will try to provide a plan with some probability to fail. In this domain we set the horizon to 6 and we will keep the initial state distribution fixed.

We do not observe the charge, but we know that the history of pl constitutes d-set for the influence sources a_{sat} . So we try to predict the influence $I^t(a_{\text{sat}}^t | (pl^0, \dots, pl^t))$ at time t based on the history of pl up to time t .

For this approximation we train a LSTM neural network (NN) [19] up to 15 epochs with 10000 samples drawn from an exploratory random policy for the rover. At each train time the NN sees the full history of plans (pl^0, \dots, pl^h) and predicts an approximate influence point $\{\hat{I}^t(\cdot | pl^0, \dots, pl^t)\}_{t=0:h}$.

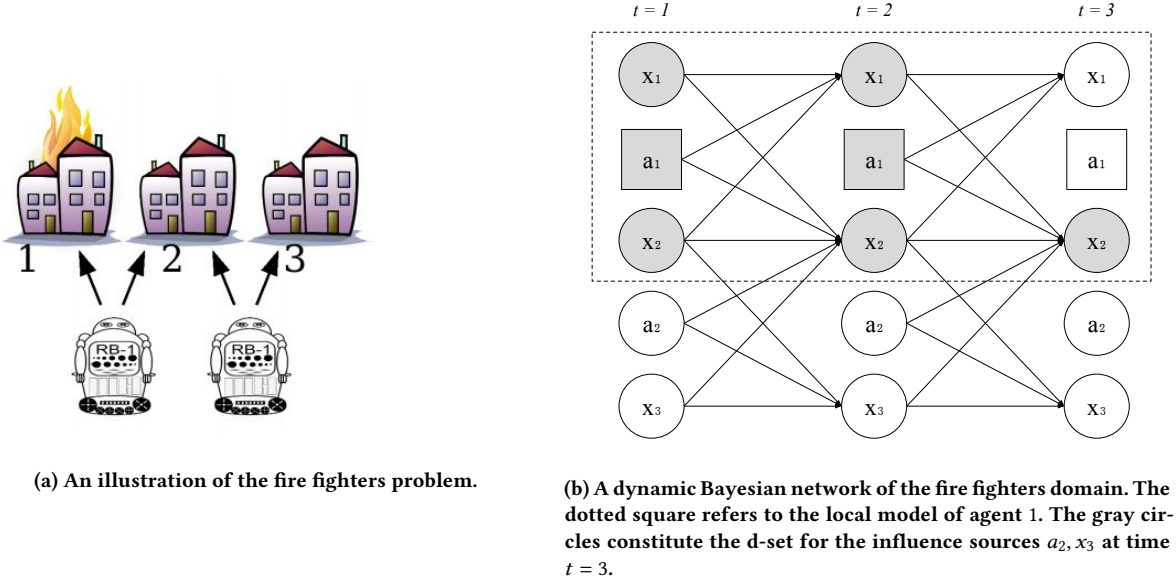


Figure 7: Fire Fighters.

B.2 Traffic Network

We simulate a busy traffic network with 4 lanes and 4 traffic light agents at the intersections (see Figure . in the main text). At every time step, each agent observes the state of a 3×3 grid around the intersection. We consider the traffic light at position (1, 1) as the local agent. We employ fixed policy for the other 3 agents. Precisely, agent (1, 4) and agent (4, 1) prioritize the horizontal lane whenever there is a vehicle waiting. For the agent in (4, 4) we use a random policy. The local space of the agent will be then composed by the observations at each side of the intersection $x = (\text{south}, \text{east}, \text{north}, \text{west})$, for $\text{south}, \text{east}, \text{north}, \text{west} \in \{0, 1\}$ where 1 corresponds to a vehicle and 0 to none. The local agent can then decide to prioritize the horizontal or the vertical lane $a_{loc} \in \{\text{hor}, \text{vert}\}$. Then, it will receive a local reward corresponding to the number of cars waiting at the intersection $R(x) = -\text{east} - \text{north}$. The outgoing vehicles from *west* and *south* have some probability to re-enter in the system from the parallel lane and then affect the other agents decisions. In this domain we set the horizon to 4 and we will keep the initial state distribution fixed. The only information the local agent needs to retrieve from the rest of the model is whether a car will access the local model from the incoming lanes. That is $X_{\text{dest}} = (\text{east}, \text{north})$. To predict incoming cars, the information the agent needs is the history of outgoing cars from *south* and *west*, $D^t = ((\text{south}^0, \text{east}^0), \dots, (\text{south}^t, \text{east}^t))$. We For this approximation we train a LSTM NN up to 16 epochs with 10000 samples drawn from a exploratory random policy for the local agent. At each training time the NN sees the history of the (*south*, *east*) and predicts the distribution of $(\text{east}^t, \text{north}^t)$.

B.3 Fire Fighters Problem

In the Fire Fighters problem [29], we model a team of 2 agents that have to extinguish fires in a row of 3 houses. At every time step, each agent can choose to fight fires at each of its neighboring houses (see Figure 7(a)). The actions of the two agents are denoted by $a_1, a_2 \in \{0, 1\}$. The state space consists of three binary factors $x_1, x_2, x_3 \in \{0, 1\}$, one for each house, where 1 indicates a burning house. Thus, a state corresponds to an assignment of the tuple $s = (x_1, x_2, x_3)$. If a house is not burning and no fire fighting agent is present with probability 0.9 the fire can spread from a neighboring house. A single agent present at a house will succeed in extinguishing the fires with probability 1 if none of the neighboring houses are burning and with probability 0.6 otherwise. If two agents fight fires at the same house, they extinguish the fire with probability 1.

We consider a local model for agent 1. It can observe only its neighboring houses x_1, x_2 and receives a reward according to the number local houses that are burning at the next time step $R(s') = -x'_1 - x'_2$. Figure 7(b) shows an illustration of the dynamic Bayesian network. In this domain we set the horizon to 4 and we will keep the initial state distribution fixed.

The local agent does not observe the state of house x_3 , therefore it can not predict the action of the non-local agent a_2 . However, the history of factors x_1, x_2 , action a_1 constitute the d-set for the influence sources a_2, x_3 . So we try to predict the influence

$I^t(a_2^t, x_3^t \mid (x_1^1, a_1^1, x_2^1, \dots, x_1^{t-1}, a_1^{t-1}, x_2^{t-1}, x_2^t))$ at time t .

For this approximation we train a LSTM NN up to 20 epochs with 100000 samples drawn from a exploratory random policy for the local agent 1. At each training time the NN sees the history of the houses x_1, x_2 and the actions taken by the local agent a_1 and predicts an approximate influence point $\{\hat{I}^t(\cdot \mid (x_1^1, a_1^1, x_2^1, \dots, x_1^{t-1}, a_1^{t-1}, x_2^{t-1}, x_2^t))\}_{t=0:h}$.

C ADDITIONAL RESULTS

Figure 8 and Figure 9 shows further results on the Planetary rover exploration domain. Precisely they present the value, test errors and correlations for the rover best response against two different policies of the satellite agent. In Figure 8, the satellite is randomly deciding at any time step to provide or not a plan. In Figure 9 the satellite decides deterministically to provide a plan whenever the level of the battery is lower than a given threshold. In both cases, the performances of the approximate-influence policy $\hat{\pi}^*$ improve with the training epochs and the cross entropy error is highly correlated with the value loss.

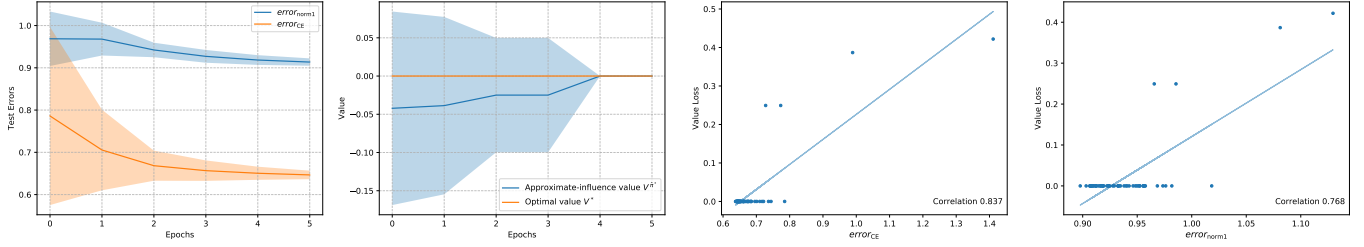


Figure 8: Random policy of the satellite

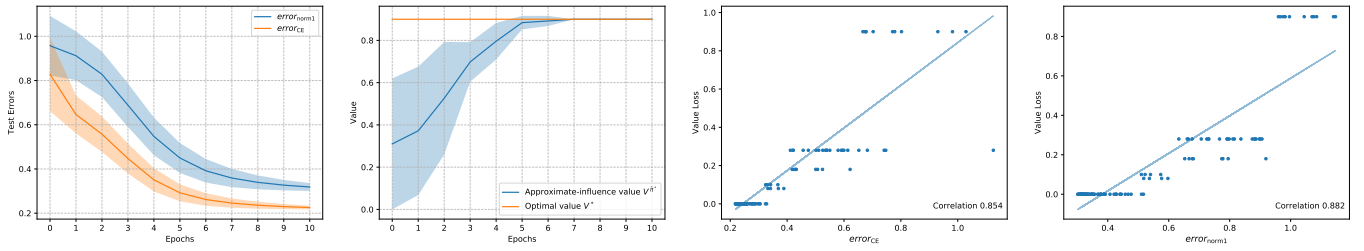


Figure 9: Deterministic policy of the satellite.